

UAV-BIM-BEM: An automatic unmanned aerial vehicles-based building energy model generation platform

Haojie Guo ^a, Zhihua Chen ^a, Xi Chen ^b, Jingjing Yang ^a, Chengcheng Song ^a, Yixing Chen ^{a,c,*}

^a College of Civil Engineering, Hunan University, Changsha 410082, China

^b Department of Mechanical and Automation Engineering, The Chinese University of Hong Kong, Shatin, NT, Hong Kong, China

^c Key Laboratory of Building Safety and Energy Efficiency of Ministry of Education, Hunan University, Changsha 410082, China

ARTICLE INFO

Keywords:

Unmanned aerial vehicles
Building energy model
Retrofit analysis
AutoBPS
Existing building

ABSTRACT

Many existing and aging buildings were in urgent need of upgrades and renovations, but lack accurate geometric and energy consumption information. This study introduced an unmanned aerial vehicles-based (UAV-based) automated platform for building information modellings (BIM) to generate building energy modellings (BEM), which was called the UAV-BIM-BEM platform. The platform enabled the creation of energy models for existing buildings to estimate energy consumption and perform retrofit analysis. A four-story office building in Hong Kong, with dimensions of 52.3 m in length, 14.3 m in width, and 16.5 m in height, was selected as the case study building. Firstly, using UAV oblique photography techniques and path planning algorithms, the building images were transformed into a detailed 3D point cloud model. The point cloud model was provided to Revit to generate the BIM model in IFC format. The IFC file containing the geometric information of the building was then supplied to the AutoBPS-BIM tool, resulting in the generation of the BEM model in EnergyPlus to simulate detailed end-use energy consumption. The annual electricity use intensity (EUI) of the building was estimated to be 145.05 kWh/m². Lastly, the generated energy model was used to evaluate the energy-saving potential of three different measures. The results showed that the electrical energy savings from cooling equipment, lighting systems, and window replacement are 17.22 %, 6.91 %, and 6.61 %, respectively. This research demonstrated that the UAV-BIM-BEM platform has great potential in BEM modeling for existing buildings and building energy retrofitting.

1. Introduction

In recent decades, the growth of the population and the continuous improvement of life quality gradually increased the energy consumption of buildings [27]. According to data provided by the International Energy Agency, in 2023, the operation energy consumption and emissions of buildings accounted for 30 % of global final energy consumption and 26 % of global energy-related emissions (8 % were direct emissions from buildings, and 18 % were indirect emissions from the production of electricity and heat used in buildings). As a result, many countries and cities were working to improve the energy efficiency of existing buildings and reduce greenhouse gas emissions [1]. Currently, many existing and aging buildings were in urgent need of upgrading and retrofitting [14]. Some existing buildings lost or did not have their design drawings, and it was hard to obtain their detailed building information, which made it difficult to carry out the subsequent building energy simulation and energy-saving retrofit process [26]. It made the subsequent building

energy simulation, as well as the energy saving retrofit process, difficult [13].

In recent years, UAVs carrying thermal cameras were increasingly used in the construction sector [35]. By harnessing the capabilities of UAVs, professionals were able to perform thorough facade inspections of buildings during on-site exploration and construction endeavors [23]. This utilization of UAV technology offers distinct advantages, including the mitigation of safety risks, enhanced detection efficiency, and the facilitation of efficient data acquisition pertinent to the characteristics of the building [7]. Tan et al. [24] proposed an automated building surface inspection method that combines UAVs with BIM, which was used to achieve high-quality and accurate inspection data collection of building surfaces. Zhang et al. [34] proposed a method for an automated building facade inspection framework supporting UAVs by matching the building facade components in the BIM model and UAV images and registering and aligning the UAV images to the BIM. The proposed method had the potential to facilitate building facade inspection by UAVs, as confirmed

* Corresponding author at: College of Civil Engineering, Hunan University, Changsha 410082, China.

E-mail address: yixingchen@hnu.edu.cn (Y. Chen).

by computer simulations and field experiments. Liu et al. [17] proposed a way to integrate the UAV inspection platform with the BIM of the building in question, driving the BIM to navigate along with the aerial video during the inspection process to accomplish the UAV inspection of the target building. Chen et al. [3] proposed a two-step program based on GIS to simplify the management process of UAV-captured images, aiming to support facade inspections of buildings.

With the help of UAVs carrying Lidar or high-resolution cameras, image collection and scanning of the interior and exterior of buildings to accomplish 3D reconstruction of indoor and outdoor scenes became a hot topic nowadays [20]. For the narrow space indoors, researchers generally used smaller and well-protected UAVs. For example, Gao et al. [8] proposed a UAV-based exploration-exploitation system for autonomous data capture and scene reconstruction of indoor facilities. Gao et al. [10] proposed a new method for indoor scene capture and reconstruction using micro UAVs and ground robots, which took into account both the completeness of the capture and the accuracy of the reconstruction. For a single large building or a cluster of urban buildings, 3D scene reproduction can be accomplished by using a UAV to acquire building point clouds or aerial images of the building [28]. Yoon et al. [31] proposed an automatic building 3D modeling framework using UAV and GCS data. The framework utilized algorithms based on You Only Look Once Version 5 (YOLOv5), Haversine's formula, UAV, and Geographic Information System (GIS) information to collect Geographic Coordinate System (GCS) data, and the collected GCS data was used to generate the EnergyPlus 3D model. Lee et al. [15] proposed a method for 3D urban reconstruction based on mobile mapping system (MMS) point clouds and oblique image enhancement of low-cost UAV photogrammetric point clouds. Yoon et al. [32] proposed an automated 3D modeling method based on UAV flights and image analysis with CNN. Shang and Shen [22] proposed a new UAV path planning method for creating high-quality 3D reconstruction models of large and complex structures.

With the increasing attention and development of methods for BIM based BEM [9], a number of BIM-based BEM methods were developed and used in practice, with commonly used methods including real-time connection, standardized exchange formats and middleware corrective tools, and proprietary tool-chain[5]. For example, Carrasco et al.[2] performed an energy simulation of a public building in Costa Rica using Autodesk Insight cloud installed in a Revit plug-in to get the thermal load of the building. Montiel-Santiago et al.[19] used the Revit plug-in Insight 360 to perform an energy simulation of the University Hospital of Jaén and to analyze. Ying et al. [30] proposed a new method that used multiple geometric representations of building elements and spaces in the industry foundation classes (IFC) model to compute the geometric and semantic information of second-level space boundaries, which solved the problem of addressing the limitations of the existing algorithms in generating the second-level space boundaries of complex buildings, and thus significantly improved the efficiency and accuracy of the automatic extraction of the BEMs from the BIM. Ramaji et al. [21] proposed an IFC-based BIM to BEM model conversion algorithm that could convert building information models represented in IFC files to building energy models in OpenStudio data format. Mediavilla et al.[18] proposed a method based on graphical techniques to automate the data exchange between BIM and BEM tools by highly reducing the need for input BIM found in similar methods, applicable to almost any IFC. Li et al.[16] proposed a new IFC-based algorithm that utilized the state-of-the-art Data-Driven Reverse Engineering Algorithm Development (D-READ) methodology and invariant signatures of HVAC objects, which was capable of converting HVAC data from BIM to BEM that addresses the research gap in HVAC interoperability between BIM and BEM. Utkucu et al. [25] used BIM as a basis to set parametric relationships of sample building elevations using Dynamo through the Revit API to enable the assessment of building energy performance.

Based on the above background, this study proposed to develop a UAV-BIM-BEM platform which was intended to have the following

innovations:1) A novel UAV-based automated modeling methodology that could set up model parameters in compliance with Chinese building standards was proposed. 2) The BIM-BEM tool in this study was possible to provide energy consumption results for individual thermal zones compared to generating BEMs using BIM plug-in. 3) The BIM-BEM tool in this study was not dependent on proprietary software compared to BIM-BEMs using APIs. 4) Compared to the existing BIM-BEM using a standardized exchange format, the BIM-BEM tool in this study does not require manual model simplification for buildings with complex shapes and structures.

This study aimed to develop a UAV-BIM-BEM platform for rapidly generating BEMs of existing buildings. The platform combined the 3D reconstruction of a building with the help of UAV and BIM to BEM modeling methods to automatically generate the BEM of the target building, including buildings with attached wall columns or other rectangular protrusions outside. Firstly, a point cloud was generated from the building images obtained from the UAV. Secondly, a BIM was manually created based on the point cloud, and finally, a BEM was generated based on the BIM, and the BEM model loads were used for usability assessment. The BEM was automatically generated for an office building in Hong Kong as a case study. Based on the generated BEM model, three different energy-saving retrofit measures were selected to analyze the building energy-saving retrofit potential.

2. Methods

Fig. 1 showed the overview of the UAV-BIM-BEM workflow in three steps. Step (1) involved scanning the existing building to obtain a detailed 3D point cloud model using a UAV. Images of the target building were captured using UAV oblique photography techniques and sent to 3D reconstruction software to generate a rough 3D point cloud model of the building. According to the rough 3D point cloud model, the area was divided, and the detailed 3D point cloud model of the building was obtained by using the UAV with the coverage path planning technology. Step (2) involved generating a BIM of the building based on the obtained detailed 3D point cloud model of the building. The detailed 3D point cloud model of the building was provided to ReCap Pro and Revit, and the geometric structural information of the building was processed to get the BIM of the target building. Step (3) focused on converting the BIM into BEM as an EnergyPlus model. The IFC file exported from Revit was provided to the AutoBPS-BIM, a rapid building modeling tool developed by Hunan University, China [4]. The AutoBPS-BIM tool extracted the necessary IFC elements for generating the geometry information for the EnergyPlus model, including building stories, space geometry boundaries, window-to-wall ratios, and space types. The EnergyPlus model for the target building was generated using AutoBPS-BIM based on the basic building information, including the building geometry, building type, year built, and climate zone. The generated EnergyPlus model was then used to perform a retrofit analysis of the building with the help of AutoBPS-Retrofit.

2.1. Simulation tools

In this study, the UAV-BIM-BEM platform was used to obtain building energy models for existing buildings as shown in **Fig. 1**, the use of the platform was divided into 3 steps.

Step (1) was to generate a point cloud model from the building images obtained from the UAV. For this part DJI Terra was used as a point cloud generation tool. It is a photogrammetric technology-centered 3D reconstruction software developed by DJI. DJI Terra can support all kinds of visible light with accurate and efficient 2D and 3D reconstruction and data processing of DJI LIDAR.

Step (2) was to manually build a BIM model based on the point cloud using Revit and ReCap Pro. Revit is a BIM software developed by Autodesk. It is one of the most widely used BIM software and can be used to perform building design, analysis and documentation. It also supports

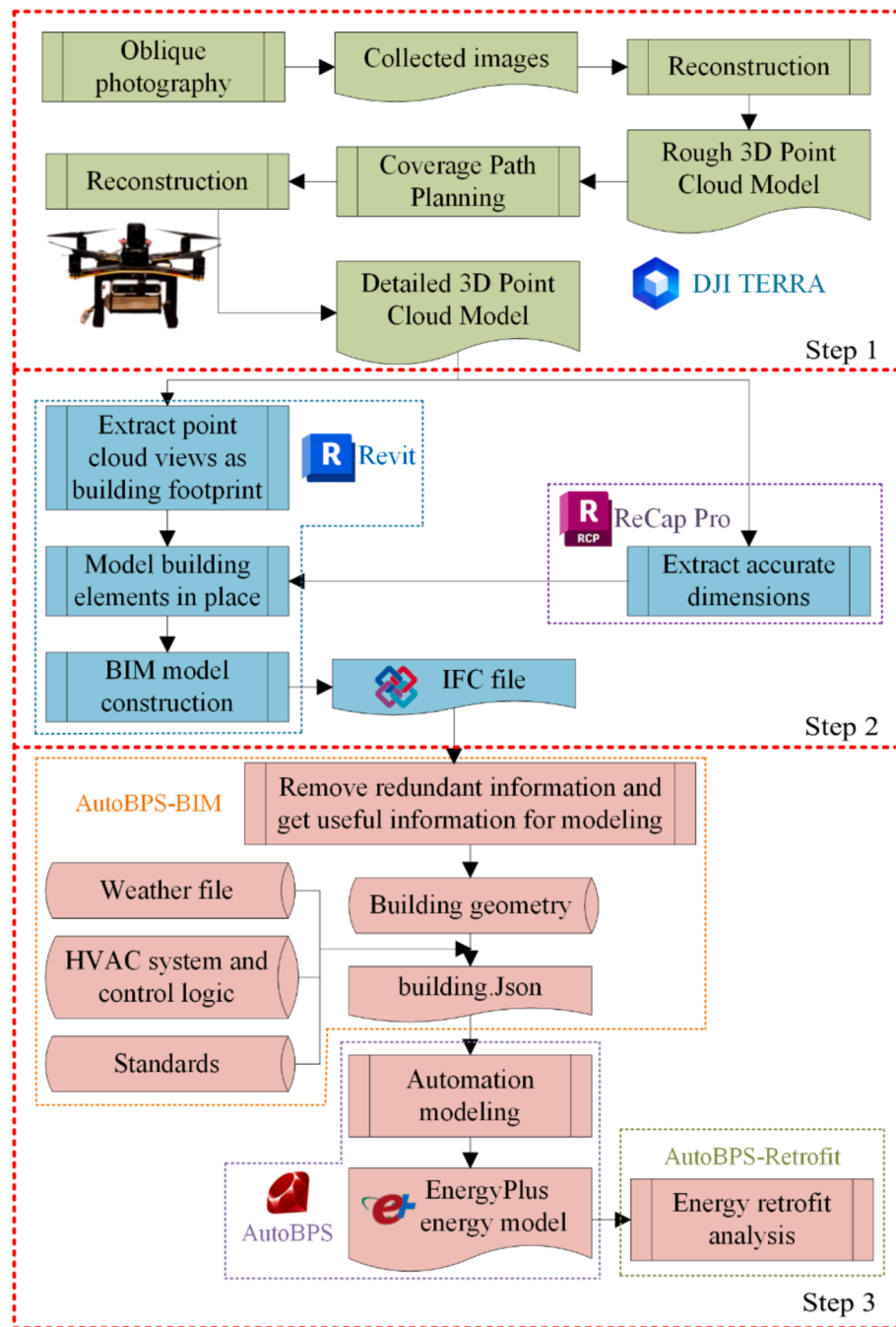


Fig. 1. Overview of UAV-BIM-BEM workflow.

exporting the BIM-BEM process in IFC or gbXML file format for BEM modeling. ReCap Pro is also one of the software programs developed by Autodesk, which can deliver a point cloud or mesh in support of BIM processes and collaborate across teams with real-world context.

Step (3) was BIM model to BEM model and energy simulation. The core of this module was AutoBPS and AutoBPS-BIM. AutoBPS-BIM was used for building energy modeling, enabling the conversion of IFC files to IDF files in the BIM-BEM process. AutoBPS is a platform for automating the energy modeling process, which is developed by Hunan University based on OpenStudio-Standards (OSS). AutoBPS has five levels of methods to rapidly generate energy models for single buildings or building clusters at urban scale. For example, Deng et al. [6] used AutoBPS to generate urban building energy models in a downtown district of Changsha and analyzed energy retrofit and rooftop

photovoltaic potential. Yang et al. [29] used AutoBPS to generate prototype building energy models and analyzed the building energy consumption and operational carbon emissions of different types of buildings in different cities. Ji et al. [11] established urban building energy models with AutoBPS and analyzed 32,145 residential buildings in Changsha City for comprehensive retrofitting with different energy-saving measures.

The last simulation tool was EnergyPlus, which is a building energy simulation tool developed by the U.S. Department of Energy (DOE). EnergyPlus was used as the core simulation engine of the AutoBPS. The building energy simulation process was accomplished through EnergyPlus.

As shown in Fig. 2, the platform was performed using four simulation tools.

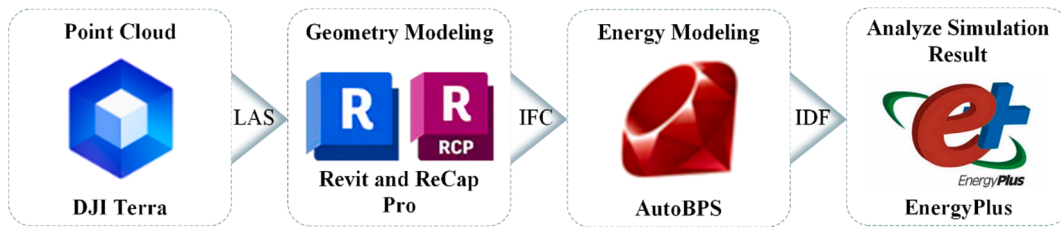


Fig. 2. Simulation process.

2.2. UAV to BIM

For the UAV to BIM portion, this study primarily employed a UAV 3D scene reconstruction technique based on a coverage path planning algorithm developed by Gao et al. [8] and a semi-automated point to BIM approach. This part mainly contained two steps to obtain the 3D point cloud of the building through the UAV and one step to generate the BIM model of the building from the 3D point cloud. The acquisition of the 3D point cloud of the building included an exploration phase and a exploitation phase, and the BIM generation from the 3D point cloud was the application phase.

During the exploration stage, the objective was to conduct data collection for 3D scene reconstruction and obtain a rough 3D point cloud model of the building. The process began with on-site field exploration, where a UAV was used to capture images of the building's external envelope from various angles through oblique aerial photography. The images collected by the UAV are then sent to the 3D reconstruction software (i.e., DJI TERRA) to generate a 3D point cloud model of the building. This process results in a rough 3D point cloud model of the building, which may had some missing details but was sufficient to meet the requirements for subsequent coverage path planning. Fig. 3 showed the rough 3D point cloud model of the building reconstructed using DJI TERRA.

In the exploitation stage, the aim was to collect more detailed data to obtain a detailed 3D point cloud model of the building. The UAV utilized a coverage path planning algorithm, which divided the target building into different regions based on the rough 3D point cloud model of the building. The algorithm down-sampled the point cloud and determined the UAV's flight route through the Traveling Salesman Problem (TSP) solver to obtained the optimum reconstructability. The TSP solver computed the coordinates of the given target points so that the UAV could visit those target points in the shortest time. The flight route of the UAV was determined, and the detailed 3D point cloud model of the

building was obtained by using DJI TERRA.

In the application stage, the detailed 3D point cloud model of the building was provided to ReCap Pro and Revit software. ReCap Pro was responsible for extracting accurate dimensional information from the building and providing it to Revit. Revit aligned the building point cloud data with the computer's coordinate system through shared coordinates for subsequent analysis, processing, visualization, and other operations. The building point cloud data was used to configure viewpoints and display levels. Point cloud views were extracted to outline the building's contours. Combining the extracting accurate dimensional information provided by ReCap Pro, the building elements were placed in specified positions for appropriate modeling to generate the building's BIM model in the IFC format. Fig. 4 displayed the 3D BIM model obtained through the 3D point cloud model.

2.3. BIM to BEM

The process of BIM to BEM through a tool called AutoBPS-BIM was shown in Fig. 5. AutoBPS-BIM was a tool developed based on AutoBPS. The core module of AutoBPS was AutoBPS-OSS, which generated an EnergyPlus model based on a prototype building model. AutoBPS-OSS required several parameters for modeling, including the building type, building standards and climate zone. There were 22 prototype building types, such as, Hospital, Large Hotel, Large Office, Primary School, Highrise Apartment and Warehouse. The core module provided the relevant prototype building geometry model from the dataset based on the building type and set up the envelope, internal gains, HVAC system and control logic of the prototype building based on the building standards and climate zones. It provided a new method for generating the geometric shape of a building based on IFC files rather than predefined prototype building geometries. This method first required converting the building information model in RVT format using Autodesk Revit 2024 as the BIM engine into the IFC2x2 format. The resulting IFC file was then provided to the AutoBPS-BIM tool, which extracted data corresponding to different parameters (such as building height, storey height, space boundary coordinates, space types, window-to-wall ratios, etc.) from the file to obtain the geometric model of the building. Using the AutoBPS-OSS integrated module, a building energy model corresponding to the actual building is obtained according to the relevant standards. The tool allowed the modeling of each floor separately. For floors with the same layout and functional type, AutoBPS-BIM enabled users to model a representative floor and use floor multipliers to scale the results. Overall, AutoBPS-BIM successfully transferred information from IFC files to energy consumption models while preserving the geometric details of the building.

The generation of the BEM model contained two parts: the geometric model and the non-geometric model. The geometric model was provided by AutoBPS-BIM. The non-geometric model was assigned to the model by selecting appropriate parameters based on building type, vintage and climate zone through building energy efficiency standards for different climate zones saved inside AutoBPS.

The previous version of the AutoBPS-BIM tool was only applicable to BIM files drawn by Revit version 2023 and below and converted to IFC2 × 2 files by Revit 2023 software and did not support IFC2 × 2 files provided by Revit software above version 2023. Additionally, the



Fig. 3. Rough 3D point cloud model of the building.

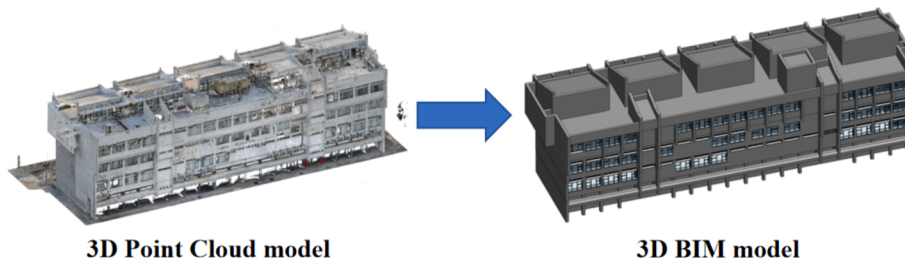


Fig. 4. 3D Point Cloud model to 3D BIM model.

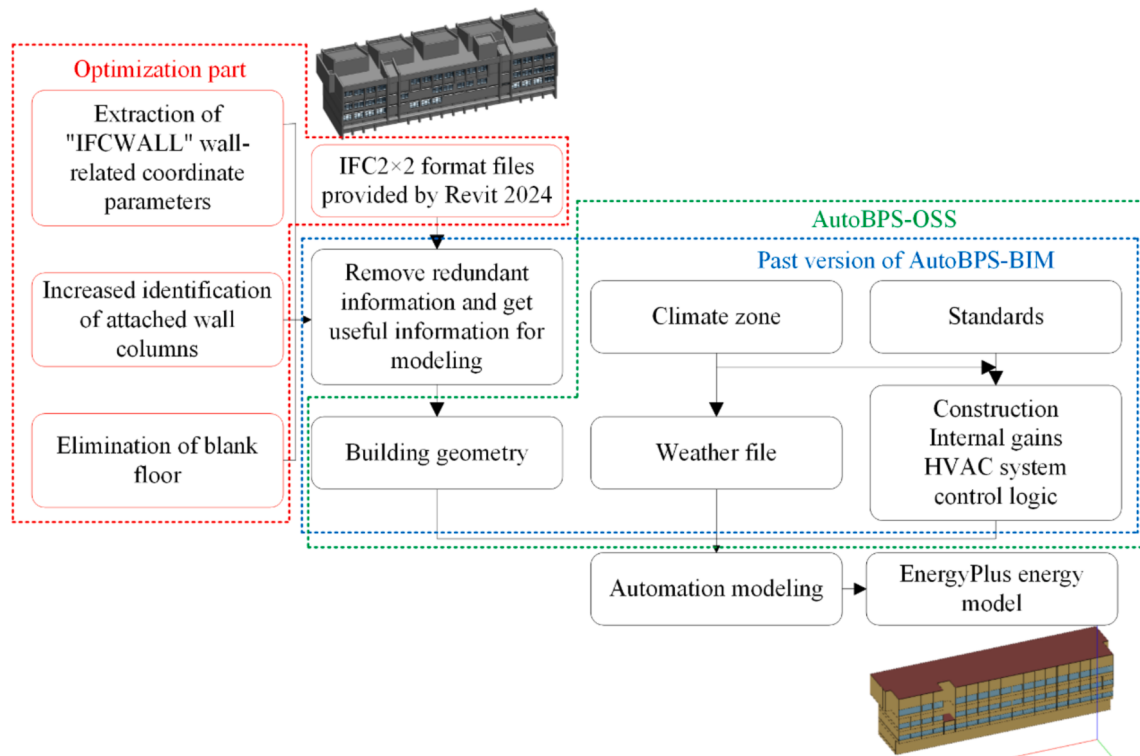


Fig. 5. Workflow of the AutoBPS-BIM tool.

previous tool could only be used for rectangular buildings with smooth and regular exterior walls; for some buildings with irregular exterior walls, there was a big difference between the BEM obtained through the past AutoBPS-BIM and the reality, which had a big impact on the generation of the building envelope. For the identification of the walls of the target building, the original tool lacked the extraction of the coordinate parameters related to the wall containing the field "IFCWALL" in the IFC file, which made it impossible to generate a complete BEM model for some buildings containing this field, the results with and without the corresponding field extraction were shown in Fig. 6.

On this basis, this study added the extraction of the coordinate parameters of the wall containing the field "IFCWALL" in the IFC file, and solved the problem that the original tool will generate a blank layer without room during the process of extracting relevant parameters from the IFC file generated by Revit 2024, thus caused the failure of the target building BEM output. Meanwhile, based on the original tool, the accuracy of the BEM output improved for buildings with irregular shapes and externally attached walls and columns. However, the accuracy of the output cannot be achieved for buildings with domes or spherical parts. The boundary smoothing function was added to eliminate the sharp corners of the space boundary by calculating the angle of each line segment in the spatial boundary, which made the BEM model more reasonable, and the process was shown in Fig. 7.

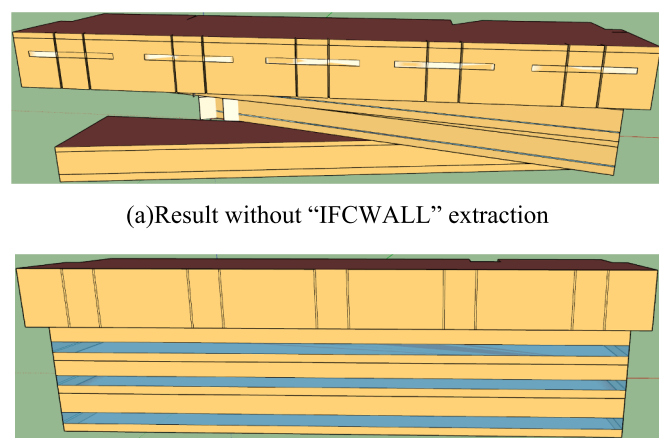


Fig. 6. Results with and without "IFCWALL" extraction.

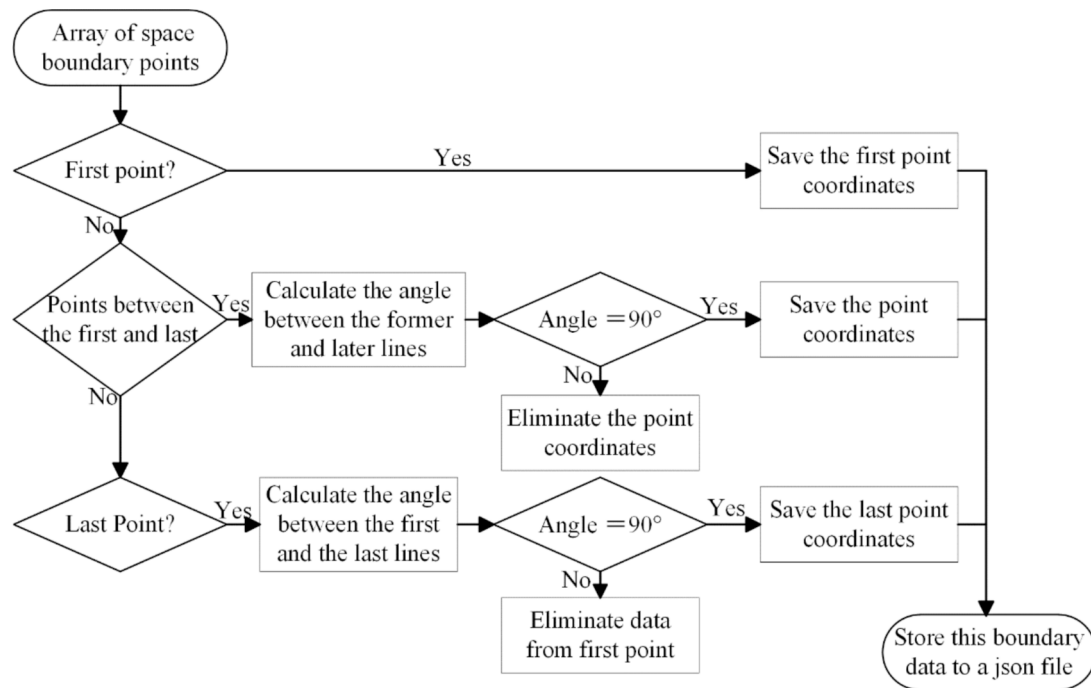


Fig. 7. The process of boundary smoothing.

The case building for this research was an office building located in Hong Kong, constructed in 1973. Due to its earlier construction year, the relevant regulations of *the Design standard for energy efficiency of public buildings* (GB50189-2005) issued by the Ministry of Housing and Urban-Rural Development (MOHURD) of the People's Republic of China were used as the reference standards for energy consumption simulation in this study. The BEM results obtained from BIM were shown in Fig. 8.

2.3.1. Climate data

The building in this study was located in the Hong Kong region, which has a hot summer and warm winter climate zone. For the simulation, the meteorological elements used for this office building were the Typical Meteorological Year (TMY) data for the Hong Kong region. TMY is a collation of long-term weather data that holds hourly solar radiation values and meteorological elements for a one-year period at a specific location. The updated TMY database was freely available on the website (<https://climate.onebuilding.org/>).

2.3.2. Envelope information

The office building in this study had four floors without a basement. The building envelope information set according to GB50189-2005 was shown in Table 1.

The windows were installed using a simple Glazing setup, and their heat transfer coefficients were shown in Table 2.

Table 1
Envelope materials of the building and their parameters.

| Category | Parameters | Value |
|--------------|--------------------------------------------------|-------|
| Construction | U-value of roof (W/(m ² ·K)) | 0.4 |
| | Roof solar reflection coefficient | 0.3 |
| | U-value of external wall (W/(m ² ·K)) | 0.45 |

Table 2
Parameters' setting of simple glazing window.

| | U-Factor (W/m ² ·K) | Solar Heat Gain Coefficient (W/m ² ·K) | Visible Transmittance |
|------------------|--------------------------------|---------------------------------------------------|-----------------------|
| Simple Glazing 1 | 2.38 | 0.34 | 0.37 |
| Simple Glazing 2 | 2.56 | 0.33 | 0.36 |
| Simple Glazing 3 | 2.40 | 0.40 | 0.15 |

2.3.3. Indoor zoning and thermal disturbance

In this study, the zoning method used for the building was to have one thermal zone per floor in order to obtain a year-round load profile at the building level, which consisted of four floors with a total of four thermal zones. The reason for adopting this zoning method was that the Hong Kong region where the case building was located was mainly

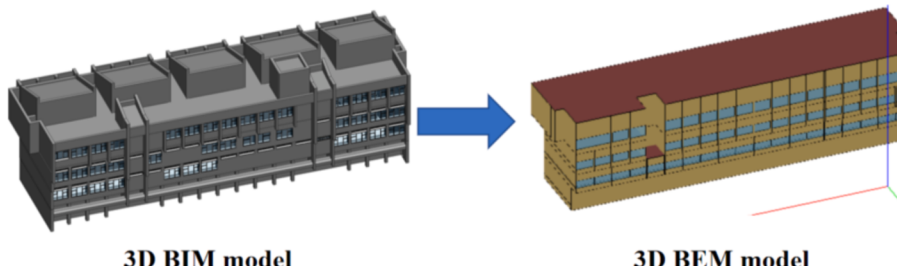


Fig. 8. Geometry of case building in BIM and BEM.

cooling-based, so heating was not considered and there was no heating load. Therefore, the hot and cold offsets did not exist, and one thermal zone per floor was acceptable. However, the zoning method was more limited, and automatic zoning needed to be developed again subsequently.

The indoor heat gains in each zone of this office building were approximately the same. According to the Chinese standard GB50189-2005, the requirements for personnel density for buildings constructed in the 1980 s, as well as the requirements for other internal heat gains, were as follows: a personnel density of $4 \text{ m}^2/\text{person}$, equipment power density of 20 W/m^2 . The building had been retrofitted and replaced as the general service life of lighting is ten years, while its lighting power density was 9 W/m^2 according to the requirements in the Chinese GB50189-2015 standard.

2.3.4. Outdoor thermal disturbance

There were two main aspects of outdoor thermal disturbances in buildings: elevators and outdoor lighting. For the energy standards of these two aspects, referred to the U.S. Department of Energy Commercial Reference Building Models of the National Building Stock published by Lawrence Berkeley National Laboratory, Pacific Northwest National Laboratory, and National Renewable Energy Laboratory. Stock. This office building had only one elevator, and the mechanical efficiency of the elevator with maximum operating floors below six is 58 %. Its specific elevator power calculation formula was shown in Equation (1).

$$\text{MotorHP} = \frac{W \cdot V \cdot [1 - OCW]}{33000 \cdot \eta_m} \quad (1)$$

Where: MotorHP is the motor power in horsepower. W is the elevator's load (lb), assuming the elevator weight is 2500 lb under the standard assumption of no overload. V is the elevator's operating speed (fpm), assuming the speed is 150 fpm. OCW is the elevator's load capacity, which is approximately 40 % for office building elevators. η_m is the elevator's mechanical efficiency.

Every exterior wall on each floor of the building and every area of the exterior wall of a single settlement was equipped with outdoor lighting. Table 3 presented the assumptions for exterior lighting in various zones according to ASHRAE Standard 90.1-1989.

2.3.5. HVAC and hot water system

The HVAC system used in each room of the office building was a split air conditioner with a cooling coefficient of performance (COP) of 2.2. The heat source of water system was a gas boiler with a thermal efficiency of 0.855. The air-conditioning was operated from 7:00 to 18:00, Monday to Friday.

2.4. Energy retrofit analysis

Improving building energy efficiency played a crucial role in promoting energy conservation, environmental protection, economic development, and social progress. Building energy efficiency could be enhanced by implementing various energy-saving technologies and management measures to improve energy utilization efficiency and reduce energy consumption in buildings. The use of UAV-based methods for automatically generating building energy models not only provided

Table 3
Exterior Lighting Assumptions.

| Area | Value of existing stock models (90.1-1989) |
|------------------------|--------------------------------------------|
| Façade | $0.25 \text{ W/ft}^2 (2.69 \text{ W/m}^2)$ |
| Main entry doors | $30 \text{ W/ft}^2 (98.4 \text{ W/m}^2)$ |
| Other doors | $25 \text{ W/ft}^2 (82.0 \text{ W/m}^2)$ |
| Canopy (heavy traffic) | $10 \text{ W/ft}^2 (108 \text{ W/m}^2)$ |
| Canopy (light traffic) | $4 \text{ W/ft}^2 (43 \text{ W/m}^2)$ |
| Parking lot | $0.18 \text{ W/ft}^2 (1.9 \text{ W/m}^2)$ |

BEM for existing buildings but also allowed AutoBPS to develop energy retrofit strategies based on the obtained BEMs. The current AutoBPS enabled the analysis of eight ECMs, including exterior walls, roofs, windows, exterior shading, air sealing, photovoltaic panels, lighting systems, and AC systems. Three specific ECMs were chosen in this research to demonstrate the potential of building performance improvement by using this platform.

Taking the Hong Kong office building in this study as an example, corresponding energy conservation measures (ECMs) were developed for its building envelope, lighting system, and air conditioning system. After obtaining the retrofit model, EnergyPlus was used as the simulation engine to calculate its EUI and as the basis for evaluating energy-saving effectiveness. Finally, energy efficiency should be selected as a key indicator to evaluate the energy-saving transformation effectiveness of the chosen ECMs.

2.4.1. Selection of ECMs

There were three main methods for energy retrofitting of existing buildings: (1) Retrofit strategies related to the building envelope, adding thermal insulation materials to the building to reduce the heat transfer coefficient of the envelope and reduce the heat loss of the building; specific measures include adding internal and external thermal insulation to the building envelope, adding the shading system, and replacing the windows with double-layer vacuum insulated glass and low emissivity (low-e) glass. (2) Retrofit strategies related to renewable energy, connecting the building with renewable energy sources such as solar and wind energy for power generation and heating. Specific measures include installing photovoltaic systems on roofs. (3) Retrofit strategies related to building systems, using more efficient energy-saving light fixtures and replacing more efficient HVAC system equipment to reduce energy consumption in buildings.

In this study, three types of ECMs were selected, and their indicators were defined according to the Technical standard for nearly zero energy buildings (GB/T 51350-2019) and the Standard for lighting design of buildings (GB 50034-2013). According to the proportion of energy consumption, the first energy-saving measure to be taken was to reduce the cooling energy consumption, and the measures that could be chosen were adopting a more efficient cooling system, reducing the use time of the cooling system, and protecting the normal operation of the cooling system, etc. Here, we adopted the replacement of the split air conditioning system as the cooling system replacement ECM.

Lighting is one of the primary sources of electricity usage in office buildings, and reducing lighting energy consumption is an important measure to improve energy utilization and reduce energy costs. Therefore, the lighting replacement ECM was used to replace the lighting system with a more energy-efficient one.

However, the building envelope also played a crucial role in achieving energy efficiency. The most commonly used methods are the retrofitting of exterior walls, roofs, and windows. Therefore, the windows replacement ECM used in this study was the replacement of window materials.

2.4.2. Energy-saving retrofit effect and economic analysis

Due to the uncertainty in analyzing ECMs during the retrofit analysis, this study adopted the energy savings rate as the indicator to measure the energy-saving effects of each ECM. The energy savings rate referred to the percentage reduction in energy consumption per unit area after the energy-saving retrofit compared to before the retrofit. Energy efficiency was calculated using Eq (2).

$$\eta = \frac{E_a - E_b}{E_b} \times 100\% \quad (2)$$

Where η is energy efficiency (%), E_a is energy consumption per unit area after the transformation (kWh/m^2), and E_b is energy consumption per unit area before the transformation (kWh/m^2).

This study employed the Payback Period (PBP) and Net Present

Value (NPV) indicators to analyze the economic feasibility. PBP is the number of years it takes for a project to repay the original investment with net income from the date of commissioning; a shorter payback period indicates lower risk and higher potential profitability. NPV is the net cash flow of an investment project after it is put into service, discounted at the cost of capital or the required rate of return for the business minus the present value of the initial investment; the magnitude of NPV indicates the level of benefits realized.

The formula was as follows:

$$PBP = \frac{C}{A} \quad (3)$$

Where C is the total cost (CNY). A is the annual net saving (CNY).

$$NPV = \sum_{t=1}^N \frac{A}{(1+i)^t} - C \quad (4)$$

Where i is the discount rate ($i = 3\%$), t is the analysis period in years. N is the remaining lifespan. A is the annual net saving.

3. Results

3.1. The results of UAV-BIM

By utilizing a UAV-based 3D scene reconstruction technique based on coverage path planning algorithms, the basic information about the building geometry could be obtained from the BIM model. As shown in Fig. 8, the office building had four floors: the heights of the first floor, second floor, third floor and fourth floor were 3.7 m, 3.1 m, 3.3 m, 3.4 m, respectively. The building had a length of 52.3 m, a width of 14.3 m and a height of 16.5 m, and the total area of the building was 2,417.67 m². The information about the area of the rooms on each floor of the building could also be viewed from the model. The model also contained geometric information for each envelope, and Table 4 showed the window-to-wall ratios (WWRs) for each orientation of the building.

Meanwhile, from the image captured by the drone in Fig. 9, it could be observed that the air conditioning systems used in the rooms on each floor of the building are all split air conditioners. The red boxes in the image highlighted the outdoor units of the split air conditioners in the rooms on each floor, as well as the outdoor components of the window air conditioners. The whole building contained a total of 120 units of split air conditioners (including window air conditioners).

Finally, the building geometry model was exported as an IFC2 × 2 format by using Revit. The IFC file contained architectural geometric information from the BIM model, such as the total area, floor heights, number of floors, WWR, and room areas. This facilitated the automatic generation of the BEM for further tasks.

3.2. Energy simulation results and model credibility assessment

The BEM was automatically generated for the office building in Hong Kong through the UAV-BIM-BEM platform, and the obtained IFC format file was provided to AutoBPS-BIM. The working hours of this office building were 07:00–18:00 on weekdays, and the results of energy consumption obtained for this office building were as follows. The monthly electricity EUI was shown in Fig. 10. Since it was an office building constructed in the early period, it had a high EUI because of its poor thermal performance and aging equipment. The annual electricity

Table 4

The window-to-wall ratio for each orientation.

| Category | Parameters | Value |
|-----------------------|------------|-------|
| Windows-to-wall ratio | South | 0.19 |
| | East | 0.008 |
| | West | 0.02 |
| | North | 0.23 |

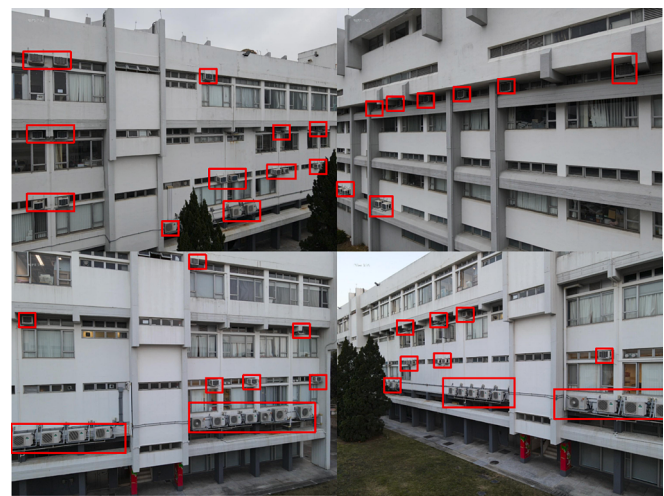


Fig. 9. Pictures of air conditioning systems.

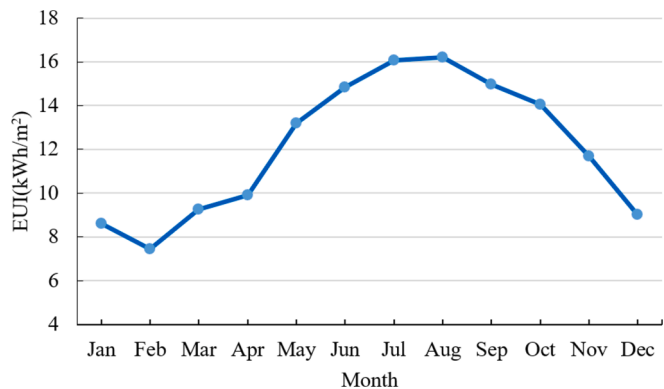


Fig. 10. Monthly electricity EUI of the case building.

consumption of the building was 350675.28 kWh, and the annual electricity consumption of EUI was 145.05 kWh/m². The annual gas consumption was 278.30 GJ, with an annual gas EUI of 0.12 GJ/m².

Fig. 11 displayed the simulated monthly electricity energy usage intensity categorized by final use. The cooling annual electricity EUI was 48.87 kWh/m², indoor lighting annual electricity EUI was 22.11 kWh/m², outdoor lighting annual electricity EUI was 12.17 kWh/m², fan annual electricity EUI was 8.50 kWh/m², and indoor equipment annual electricity EUI was 46.02 kWh/m². Outdoor equipment's annual electricity EUI was 7.36 kWh/m².

Fig. 12 showed the simulated electricity consumption results of the

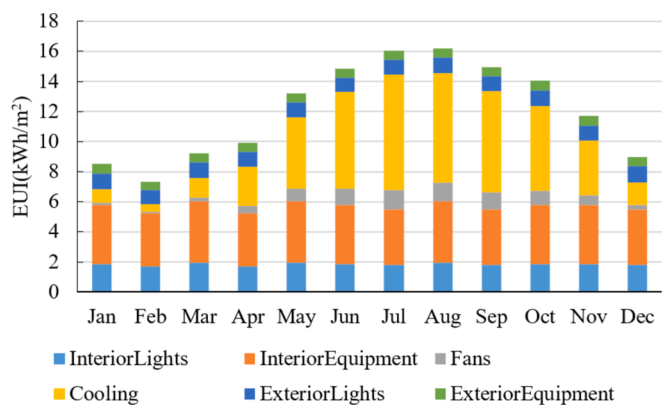


Fig. 11. Simulated monthly electrical energy consumption by end-use.

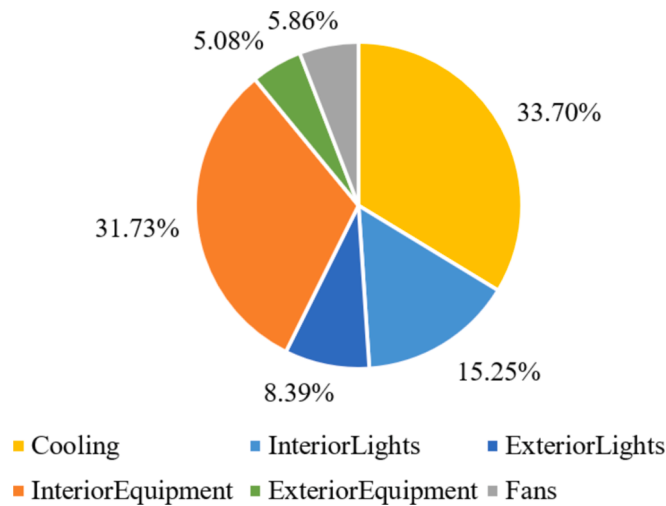


Fig. 12. Proportion of end-use energy consumption.

case study building energy model. The highest proportions of interior energy consumption were the cooling energy consumption of the chiller (33.70 %), energy consumption of interior equipment (31.73 %), and energy consumption of interior lighting (15.25 %).

In addition, the ideal cooling and heating loads for each room, each floor, and each thermal zone could be obtained from the EnergyPlus model automatically generated by AutoBPS-BIM. Since the building had one thermal zone for the entire first floor, the loads for each floor are presented here for demonstration. Fig. 13 displayed the cooling and heating design loads for first floor to fourth floor of the building. The cooling design loads for first floor, second floor, third floor and fourth floor were 51.59 W/m^2 , 57.76 W/m^2 , 59.46 W/m^2 , and 90.35 W/m^2 , respectively. The heating design loads for first floor, second floor, third floor and fourth floor were 72.12 W/m^2 , 70.86 W/m^2 , 76.56 W/m^2 , and 115.87 W/m^2 , respectively.

It was important to verify the credibility of the model results in order to conduct further research. The most commonly used method was to calibrate the building energy model based on building measured data, which required building measured data and is therefore suitable for existing buildings for which measured data was available. Since the case building of this study lacked measured building energy consumption data, an alternative approach was used to verify the credibility of the results by ensuring that the input parameters of the energy model were correct and comply with the recommended values of existing studies or building standards. Existing research survey data of buildings of the same type and similar construction year in Hong Kong were selected for model validation to ensure that the simulation results were within reasonable limits. Jing et al. [12] surveyed 30 office buildings with

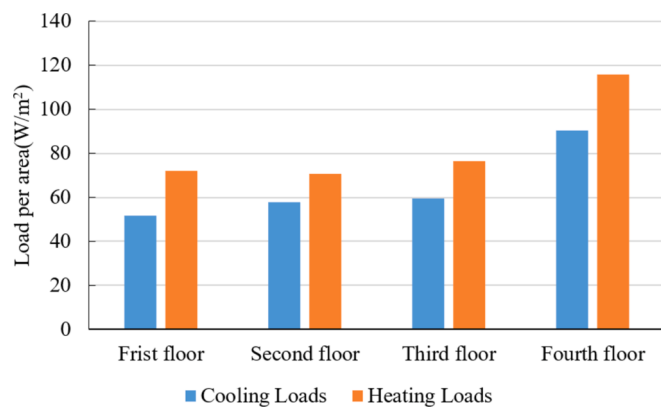


Fig. 13. Design cooling and heating loads for first floor to fourth floor.

varying floor heights ranging from 6 to 54 floors. The average annual EUI obtained was $236 \text{ kWh}/(\text{m}^2\text{-year})$, with a maximum value of $529 \text{ kWh}/(\text{m}^2\text{-year})$ and a minimum value of $74 \text{ kWh}/(\text{m}^2\text{-year})$. Yu et al. [33] based on the Hong Kong energy-use data provided by the Electrical and Mechanical Services Department (EMSD) on the EUI of office buildings in Hong Kong from 2009 to 2017, which ranged from 311 kWh/m^2 to 323 kWh/m^2 . By incorporating the above survey data, the simulation results of the automatically generated office building model were verified and found to be within the range of the measured data, ensuring that the model results were within a reasonable range.

3.3. Retrofit analysis results

For the cooling system replacement ECM, one common method in the retrofit of the cooling system was to replace the existing split air conditioning system with a higher COP value. According to the GB/T 51350–2019 Technical standard for nearly zero energy buildings, the COP of the replaced split air conditioning system was set to 4.5. In the existing office building energy model, the COP value of the model has been changed from 2.2 to 4.5 to reflect this replacement.

For the lighting replacement ECM, changing the internal lighting power density of the building was a relatively efficient method of retrofitting the lighting system. According to the GB 55015–2021 General code for energy efficiency and renewable energy application in buildings, the lighting power density of the existing office building has been changed from 9 W/m^2 to 6 W/m^2 .

For the retrofit of the building envelope, the window replacement ECM involved replacing the existing windows with more thermally insulating windows to save energy. The parameters that affect window energy consumption were mainly the U-factor (thermal transmittance) and the solar heat gain coefficient (SHGC). Therefore, in the EnergyPlus model, changing the window strategy could be achieved by modifying the U-factor and SHGC of the windows. Referred to the energy-saving measures by Deng et al. [6], the U-factor of the windows has been changed from 2.38 W/m^2 , 2.56 W/m^2 , 2.40 W/m^2 to 1.14 W/m^2 and the SHGC of the windows has been changed from 0.34, 0.33, 0.40 to 0.19. These values were chosen to reflect the improved thermal insulation and reduced solar heat gain properties of the new windows.

The annual electricity EUI for each ECM was shown in Fig. 14. The cooling system replacement ECM reduced the annual EUI of the building from 145.05 kWh/m^2 to 120.07 kWh/m^2 , resulted in an annual energy savings rate of 17.22 %. This was achieved by replacing the split air conditioning system with a higher COP. The lighting replacement ECM reduced the annual EUI of the building from 145.05 kWh/m^2 to 135.03 kWh/m^2 , resulted in an annual energy savings rate of 6.91 %. This was accomplished by replacing the lighting system with a more energy-efficient one. The window replacement ECM reduced the annual EUI of the building from 145.05 kWh/m^2 to 135.46 kWh/m^2 , resulted in an

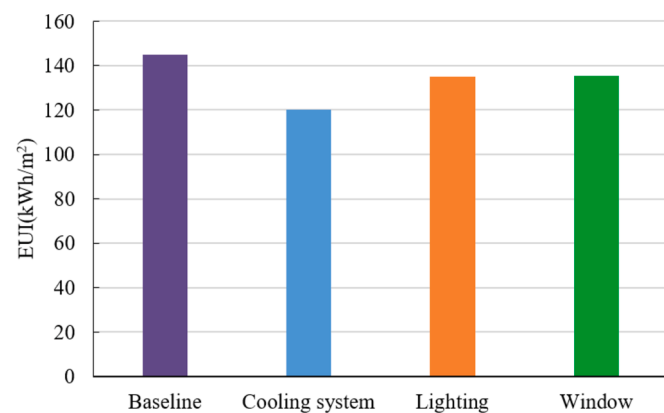


Fig. 14. Annual electricity EUI for baseline and each ECM.

annual energy savings rate of 6.61 %. This was achieved by replacing the windows with more thermally insulating glass. Retrofitting the cooling system could significantly reduce the EUI, while retrofitting the lighting system and windows saved relatively little energy.

The monthly EUI energy savings rate for each ECM were shown in Fig. 15. For this office building, the monthly energy savings rate of the cooling system replacement ECM ranged from 3.29 % to 24.37 %, and the best energy saving was in the month of July, which showed that lowering the COP significantly reduced the energy consumption of the air conditioning system in summer. There was no obvious seasonal difference between the other two ECMs, the monthly energy saving rate of the lighting replacement ECM ranged from 5.32 % to 9.02 %; the monthly energy saving rate of the window replacement ECM ranged from 2.81 % to 8.95 %.

According to the 2024 Electricity Tariff Schedule provided by China Light and Power (CLP) Holdings Limited, the non-residential electricity tariff in Hong Kong was 0.99 CNY/kWh. Conducting cost research through online shopping websites, the material costs were calculated to determine the total cost. The specific material costs were shown in Table 5.

The investment for cooling system replacement ECM was 244.86 CNY/m², with a relatively lower investment for changing the lighting system. The investment for lighting replacement ECM was only 7.5 CNY/m², while the investment for window replacement ECM is 21.41 CNY/m². Typically, the lifespan of windows and photovoltaic systems was 20 years, while the lifespan of lighting and air conditioning systems was 10 years. Fig. 16 showed the PBP of each energy-saving strategy. The PBP for cooling system replacement ECM was 13.07 years, and from the results, it could be seen that in the case of this office building, enhancing the existing air conditioning system, while capable of substantially curtailing overall energy consumption, remains economically inadvisable. For lighting replacement ECM, due to the lower total cost of replacing the lighting system, the payback period for the renovated lighting system in the building was the shortest, requiring only 1.01 years to recover the cost. The payback period for window replacement ECM was 3.01 years. Replacing both the lighting system and the windows could pay for itself before the end of its life.

According to China's *Design Standards for Office Buildings (JGJ/T 67-2019)*, the service life for particularly important office buildings was set at 100 years. This office building's remaining lifespan was 49 years. The NPV results for each energy-saving strategy were shown in Fig. 16. The NPV for cooling system, lighting and window replacement ECM were 0.74 Million CNY, 0.60 Million CNY, and 0.52 Million CNY, respectively.

All three ECMs had good energy-saving effects for this building, but while retrofitting the cooling system had better energy savings, the investment was higher. Retrofitting the lighting was the cheapest of these strategies, and the energy-saving effect was better than retrofitting the windows, so the lighting retrofitting should be considered first.

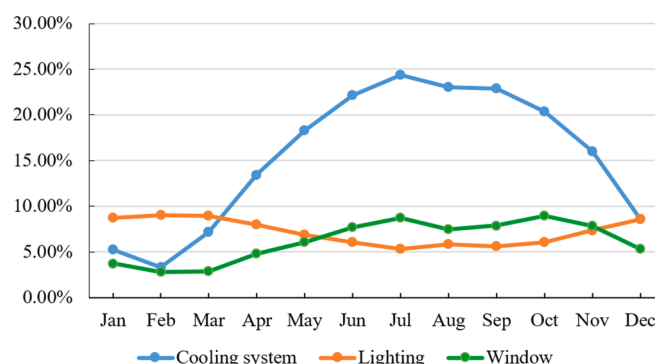


Fig. 15. Monthly energy savings rate for each ECM.

Table 5
Detailed settings of material.

| Material items | Parameters | Price |
|-------------------------------|----------------------------------------|------------------------|
| Split air conditioning system | 4.5(COP) | 3700 CNY/Piece |
| Lighting | 6 W/m ² | 7.5 CNY/m ² |
| Window | 1.44 W/(m ² ·K), 0.19(SHGC) | 110 CNY/m ² |

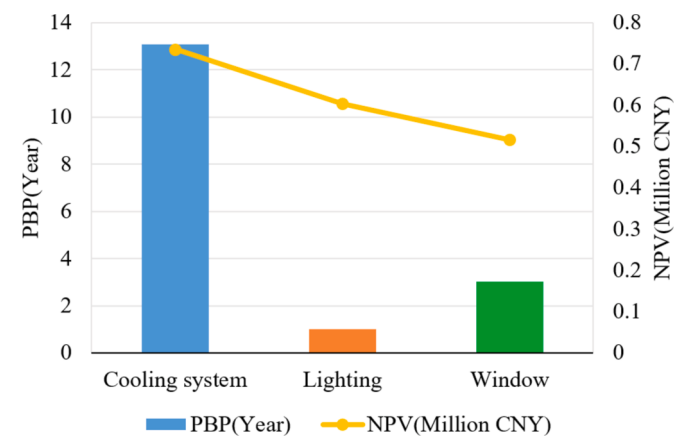


Fig. 16. The PBP and NPV results of each energy-saving strategy

4. Limitations

There were some limitations in this study. The first limitation was that due to the lack of measured data for the case buildings in this study, only the energy consumption results of office buildings located in the same region in similar years from different literature were used for model credibility validation. Meanwhile, the BEM model was generated based on prototype building, so there would be some error with the actual control and the actual form of air conditioning system. Using this method for model validation only established that the energy consumption results of the generated model were in a reasonable and credible range and were insufficient to ensure that the model was completely accurate. Also, this study did not perform a sensitivity analysis on the input parameters of the model, which helps to understand the impact of various assumptions on the accuracy of the model.

The second limitation was that the Hong Kong region was mainly cooling-based, the heating of the case building was not considered, so the hot and cold offsets did not exist. Therefore, the current tool could only set one heat zone for each floor for internal zoning of buildings. Setting multiple thermal zones on the same floor required manual configuration, which was not automated in the current tool. Adopting this zoning method impacted the energy simulation for other buildings with complex usage patterns or different internal gains, such as higher simulated energy consumption for the internal zones.

The third limitation was that the UAV-BIM-BEM platform was currently researched and developed based on China's building standards. Local building energy standards, such as provincial building energy efficiency standards, were not considered in the current AutoBPS.

The fourth limitation was that although point clouds could be obtained from UAV oblique photography for buildings featuring domes or spherical elements, subsequent BIM manual modeling based on point clouds was very complex. AutoBPS-BIM did not currently support the modeling of such buildings. Therefore, the UAV-BIM-BEM platform was not yet applicable to buildings featuring domes or spherical elements.

5. Discussion

The UAV-BIM-BEM platform is a semi-automated modeling platform. In the UAV to BIM part, using Revit and Recap Pro software to complete

the point cloud to BIM process required manual completion of BIM modeling, while all other parts could be automated. It was relatively simple to integrate the platform into existing work, and users only needed to acquire the following three professional knowledge to master the use of the platform: firstly, correctly using the UAV to complete oblique photography; secondly, being able to use point cloud data to place building elements in the building model according to the point cloud file imported into Revit; thirdly, being able to use ReCap Pro to obtain specific information about doors, windows, etc. according to the point cloud file. Using this platform to complete the semi-automated modeling of a single building can save a lot of time and energy compared to manual modeling of a single building.

This study developed a UAV-based BEM automatic generation system, which allowed for quickly acquiring BEM models for existing buildings. This enabled engineers to conveniently evaluate energy-saving retrofitting of the existing building. However, the lack of actual measured data from the case building was insufficient to ensure the model was completely accurate. In future work, we will utilize the UAV-BIM-BEM platform to create an energy model for an existing building from measured data to complete validation of the model's accuracy and perform sensitivity analyses on key parameters to understand the impact of various assumptions on the model's accuracy.

The BEM model generated by the UAV-BIM-BEM platform could output the building's electrical consumption and gas use, as well as the cooling and heating loads for each room. However, for the building's interior zoning, the current tool could only set one thermal zone per floor. Setting multiple thermal zones on the same floor required manual configuration, which was not automated in the current tool. In future research, a comprehensive review will be conducted on commercial building energy modeling standards and guidelines such as *ASHRAE 90.1–2016*, Appendix G, *IBPSA Building Energy Modeling Handbook (BEMBook)*, *CIBSE Application Manual AM11*, etc. This study will focus on further optimizing the thermal zoning of interior spaces within buildings.

This study made modifications and optimizations to the recognition of building exterior shapes compared to the previous AutoBPS-BIM tool, manual simplification of BIM models with external wall columns or regular rectangular protrusions was not required to eliminate these influencing factors in order to generate the BEM model. However, the UAV-BIM-BEM system could not accurately generate BEM models for buildings with domes or other spherical elements in its external structures. In future research, more in-depth studies will be conducted to achieve fully automated or as simple as possible BIM modeling and to develop the extraction capabilities for spherical envelopes of AutoBPS-BIM.

In summary, the UAV-BIM-BEM platform could effectively assist engineers or researchers in automating the modeling process of existing building energy models, reducing the complexity of modeling. It could also support energy efficiency potential analysis and energy performance evaluation based on the obtained models. However, the system was currently not perfect and requires further expansion of its capabilities in the future. This included adding automatic thermal zoning, adding building standards for other regions, and improving the automatic generation of BEM for buildings with spherical elements.

6. Conclusion

In this paper, an efficient UAV-BIM-BEM platform was developed. The method combined UAV scene reproduction with BIM to BEM, which could obtain a building point cloud based on a UAV and create a building information model and a building energy model of the target building. Based on the generated energy models, the proposed workflow could also provide building heating and cooling loads for each space as well as the energy consumption data for each part.

An office building located in Hong Kong was selected as the case study building in this research. The proposed platform utilized UAVs to

rapidly capture images of the building, obtained information on the walls, doors, and windows and generating a point cloud model of the building. Through modeling software, this information was stored in an IFC file. AutoBPS-BIM tool was used to quickly generate the BEM for the case study building based on BIM, and analyze the cooling and heating loads of each space and energy consumption for different systems. The annual electricity EUI of the building obtained from this system was 145.05 kWh/m². By compared the simulated results with the actual measured data of annual electricity EUI from various literature sources for office buildings in Hong Kong, the credibility of the obtained simulation results was confirmed within the range of measured data, which demonstrated a high level of reliability. Furthermore, the generated building energy model was used to evaluate three different energy-saving strategies. The results showed that the cost of retrofitting lighting was 2.76 CNY/m² and the energy saving rate was 6.91 %, the cost was the lowest among the three strategies and there was a good energy saving effect, so retrofitting lighting should be considered first.

In general, this study proposed a platform for the rapid generation of energy models of various types of buildings without featuring domes or spherical elements that comply with Chinese building standards, including single-function and multi-function buildings. The platform could be integrated into existing workflows with relative simplicity, and users only need to have a small amount of specialized knowledge (UAV oblique photography and using Revit and ReCap Pro) to use it. It could also help improve the energy efficiency of existing buildings and assists decision-makers in setting effective energy-saving and emission-reduction goals.

7. Declaration of generative AI and AI-assisted technologies in the writing process

During the preparation of this work the authors used Grammarly and ChatGPT in order to improve readability and to detect spelling/grammar mistakes. After using this tool/service, the authors reviewed and edited the content as needed and takes full responsibility for the content of the publication.

CRediT authorship contribution statement

Haojie Guo: Writing – original draft, Visualization, Software, Methodology, Data curation. **Zhihua Chen:** Writing – review & editing, Software. **Xi Chen:** Writing – review & editing, Methodology, Data curation. **Jingjing Yang:** Writing – review & editing. **Chengcheng Song:** Writing – review & editing. **Yixing Chen:** Writing – review & editing, Supervision, Funding acquisition, Conceptualization.

Declaration of competing interest

The authors declare that they have no known competing financial interests or personal relationships that could have appeared to influence the work reported in this paper.

Acknowledgements

This paper is supported by the National Natural Science Foundation of China (NSFC) through Grant No. 52478088. This work is also funded by the Key Research and Development Project of Hunan Province of China through Grant No. 2024AQ2011. Additional support is provided by “A Project Supported by the Scientific Research Fund of Hunan Provincial Education Department, China (No. 23A0033 and No. 2023JGZD027)”.

Data availability

Data will be made available on request.

References

- [1] N. Bucarelli, N. El-Gohary, Sensor deployment configurations for building energy consumption prediction, *Energy and Buildings* 308 (2024), <https://doi.org/10.1016/j.enbuild.2024.113888>.
- [2] C.A. Carrasco, I. Lombillo, F.J. Balbás, J.R. Aranda, K. Villalta, Building Information Modeling (BIM 6D) and Its Application to Thermal Loads Calculation in Retrofitting, *Buildings* 13 (8) (2023), <https://doi.org/10.3390/buildings13081901>.
- [3] K. Chen, G. Reichard, A. Akanmu, X. Xu, Geo-registering UAV-captured close-range images to GIS-based spatial model for building façade inspections, *Automation in Construction* 122 (2021), <https://doi.org/10.1016/j.autcon.2020.103503>.
- [4] Z. Chen, Z. Deng, A. Chong, Y. Chen, AutoBPS-BIM: A toolkit to transfer BIM to BEM for load calculation and chiller design optimization, *Building Simulation* 16 (7) (2023) 1287–1298, <https://doi.org/10.1007/s12273-023-1006-4>.
- [5] A. Ciccozzi, T. de Rubeis, D. Paolletti, D. Ambrosini, BIM to BEM for Building Energy Analysis: A Review of Interoperability Strategies, *Energies* 16 (23) (2023) 1–45, <https://doi.org/10.3390/en16237845>.
- [6] Z. Deng, Y. Chen, J. Yang, F. Causone, AutoBPS: A tool for urban building energy modeling to support energy efficiency improvement at city-scale, *Energy and Buildings* 282 (2023), <https://doi.org/10.1016/j.enbuild.2023.112794>.
- [7] J. Ding, J. Zhang, Z. Zhan, X. Tang, X. Wang, A Precision Efficient Method for Collapsed Building Detection in Post-Earthquake UAV Images Based on the Improved NMS Algorithm and Faster R-CNN, *Remote Sensing* 14 (3) (2022), <https://doi.org/10.3390/rs14030663>.
- [8] C. Gao, X. Wang, R. Wang, Z. Zhao, Y. Zhai, X. Chen, B.M. Chen, A UAV-based explore-then-exploit system for autonomous indoor facility inspection and scene reconstruction, *Automation in Construction* 148 (2023), <https://doi.org/10.1016/j.autcon.2023.104753>.
- [9] H. Gao, C. Koch, Y. Wu, Building information modelling based building energy modelling: A review, in: *Applied Energy*, Vol. 238, Elsevier Ltd., 2019, pp. 320–343, <https://doi.org/10.1016/j.apenergy.2019.01.032>.
- [10] X. Gao, L. Zhu, H. Cui, Z. Hu, H. Liu, S. Shen, Complete and Accurate Indoor Scene Capturing and Reconstruction Using a Drone and a Robot, *IEEE Sensors Journal* 21 (10) (2021) 11858–11869, <https://doi.org/10.1109/JSEN.2020.3024702>.
- [11] Y. Ji, G. Li, F. Su, Y. Chen, R. Zhang, Retrofit Analysis of City-Scale Residential Buildings in the Hot Summer and Cold Winter Climate Zone, *Energies* 16 (17) (2023), <https://doi.org/10.3390/en16176152>.
- [12] R. Jing, M. Wang, R. Zhang, N. Li, Y. Zhao, A study on energy performance of 30 commercial office buildings in Hong Kong, *Energy and Buildings* 144 (2017) 117–128, <https://doi.org/10.1016/j.enbuild.2017.03.042>.
- [13] D.E. Jung, S. Kim, S. Han, S. Yoo, H. Jeong, K.H. Lee, J. Kim, Appropriate level of development of in-situ building information modeling for existing building energy modeling implementation, *Journal of Building Engineering* 69 (2023), <https://doi.org/10.1016/j.jobe.2023.106233>.
- [14] S. Kaashi, A. Vilventhan, Development of a building information modelling based decision-making framework for green retrofitting of existing buildings, *Journal of Building Engineering* 80 (June) (2023) 108128, <https://doi.org/10.1016/j.jobe.2023.108128>.
- [15] E. Lee, S. Park, H. Jang, W. Choi, H.G. Sohn, Enhancement of low-cost UAV-based photogrammetric point cloud using MMS point cloud and oblique images for 3D urban reconstruction, *Measurement: Journal of the International Measurement Confederation* 226 (2024), <https://doi.org/10.1016/j.measurement.2024.114158>.
- [16] H. Li, J. Zhang, Improving IFC-Based Interoperability between BIM and BEM Using Invariant Signatures of HVAC Objects, *Journal of Computing in Civil Engineering* 37 (2) (2023) 1–20, [https://doi.org/10.1061/\(asce\)cp.1943-5487.0001063](https://doi.org/10.1061/(asce)cp.1943-5487.0001063).
- [17] D. Liu, X. Xia, J. Chen, S. Li, Integrating Building Information Model and Augmented Reality for Drone-Based Building Inspection, *Journal of Computing in Civil Engineering* 35 (2) (2021), [https://doi.org/10.1061/\(asce\)cp.1943-5487.0000958](https://doi.org/10.1061/(asce)cp.1943-5487.0000958).
- [18] A. Mediavilla, P. Elguezabal, N. Lasarte, Graph-Based methodology for Multi-Scale generation of energy analysis models from IFC, *Energy and Buildings* 282 (2023) 112795, <https://doi.org/10.1016/j.enbuild.2023.112795>.
- [19] Montiel-Santiago, F. J., Hermoso-Orzáez, M. J., & Terrados-Cepeda, J. (2020). Sustainability and energy efficiency: Bim 6d. study of the bim methodology applied to hospital buildings. value of interior lighting and daylight in energy simulation. *Sustainability (Switzerland)*, 12(14), 1–29. <https://doi.org/10.3390/su12145731>.
- [20] M. Oelsch, M. Karimi, E. Steinbach, R-LOAM: Improving LiDAR Odometry and Mapping with Point-to-Mesh Features of a Known 3D Reference Object, *IEEE Robotics and Automation Letters* 6 (2) (2021) 2068–2075, <https://doi.org/10.1109/LRA.2021.3060413>.
- [21] I.J. Ramaji, J.I. Messner, E. Mostavi, IFC-Based BIM-to-BEM Model Transformation, *Journal of Computing in Civil Engineering* 34 (3) (2020) 1–13, [https://doi.org/10.1061/\(asce\)cp.1943-5487.0000880](https://doi.org/10.1061/(asce)cp.1943-5487.0000880).
- [22] Z. Shang, Z. Shen, Topology-based UAV path planning for multi-view stereo 3D reconstruction of complex structures, *Complex and Intelligent Systems* 9 (1) (2023) 909–926, <https://doi.org/10.1007/s40747-022-00831-5>.
- [23] H. Shin, J. Kim, K. Kim, S. Lee, Empirical Case Study on Applying Artificial Intelligence and Unmanned Aerial Vehicles for the Efficient Visual Inspection of Residential Buildings, *Buildings* 13 (11) (2023), <https://doi.org/10.3390/buildings13112754>.
- [24] Y. Tan, S. Li, H. Liu, P. Chen, Z. Zhou, Automatic inspection data collection of building surface based on BIM and UAV, *Automation in Construction* 131 (2021), <https://doi.org/10.1016/j.autcon.2021.103881>.
- [25] Utkucu, D., & Sözer, H. (2020). Interoperability and data exchange within BIM platform to evaluate building energy performance and indoor comfort. *Automation in Construction*, 116(October 2019), 103225. <https://doi.org/10.1016/j.autcon.2020.103225>.
- [26] D. Wang, Q. Jiang, J. Liu, Deep-Learning-Based Automated Building Information Modeling Reconstruction Using Orthophotos with Digital Surface Models, *Buildings* 14 (3) (2024), <https://doi.org/10.3390/buildings14030808>.
- [27] H. Xi, Q. Zhang, Z. Ren, G. Li, Y. Chen, Urban Building Energy Modeling with Parameterized Geometry and Detailed Thermal Zones for Complex Building Types, *Buildings* 13 (11) (2023), <https://doi.org/10.3390/buildings13112675>.
- [28] F. Yan, E. Xia, Z. Li, Z. Zhou, Sampling-based path planning for high-quality aerial 3D reconstruction of urban scenes, *Remote Sensing* 13 (5) (2021) 1–23, <https://doi.org/10.3390/rs13050989>.
- [29] Yang, J., Zhang, Q., Peng, C., & Chen, Y. (2024). AutoBPS-Prototype: A web-based toolkit to automatically generate prototype building energy models with customizable efficiency values in China. *Energy and Buildings*, 305 (September 2023), 113880. <https://doi.org/10.1016/j.enbuild.2023.113880>.
- [30] Ying, H., & Lee, S. (2021). Generating second-level space boundaries from large-scale IFC-compliant building information models using multiple geometry representations. *Automation in Construction*, 126(June 2020), 103659. <https://doi.org/10.1016/j.autcon.2021.103659>.
- [31] J. Yoon, Y. Kim, S. Lee, M. Shin, UAV-based automated 3D modeling framework using deep learning for building energy modeling, *Sustainable Cities and Society* 101 (2024), <https://doi.org/10.1016/j.scs.2023.105169>.
- [32] J. Yoon, H. Shin, K. Kim, S. Lee, CNN- and UAV-Based Automatic 3D Modeling Methods for Building Exterior Inspection, *Buildings* 14 (1) (2024), <https://doi.org/10.3390/buildings14010005>.
- [33] Yu, F. W., & Ho, W. T. (2021). Tactics for carbon neutral office buildings in Hong Kong. *Journal of Cleaner Production*, 326(October 2021). <https://doi.org/10.1016/j.jclepro.2021.129369>.
- [34] C. Zhang, F. Wang, Y. Zou, J. Dimyadi, B.H.W. Guo, L. Hou, Automated UAV image-to-BIM registration for building façade inspection using improved generalised Hough transform, *Automation in Construction* 153 (2023), <https://doi.org/10.1016/j.autcon.2023.104957>.
- [35] C. Zhang, Y. Zou, J. Dimyadi, R. Chang, Thermal-textured BIM generation for building energy audit with UAV image fusion and histogram-based enhancement, *Energy and Buildings* 301 (2023), <https://doi.org/10.1016/j.enbuild.2023.113710>.